Prediction of Clinically Significant Prostate Cancer in MR/Ultrasound Guided Fusion Biopsy using Multiparametric MRI

Wen Shi[*]
jsnjsw97@stu.xjtu.edu.cn

Karthik V. Sarma[†]
ksarma@mednet.ucla.edu

Alex G. Raman[†]
araman@mednet.ucla.edu

Alan M. Priester[‡§]
apriester@mednet.ucla.edu

Shyam Natarajan[‡§]
snatarajan@mednet.ucla.edu

William Speier[†]
wspeier@mednet.ucla.edu

Steven S. Raman[†]
sraman@mednet.ucla.edu

Leonard S. Marks[§]
lmarks@mednet.ucla.edu

Corey W. Arnold[†¶]
cwarnold@mednet.ucla.edu

Abstract

Prostate biopsy is commonly used to detect and stage prostate cancer. However, accurate biopsy targeting requires the prior identification of appropriate targets for sampling. Imaging-based decision support systems have significant potential to improve targeting by predicting which potential biopsy locations are most likely to have cancer, and which can safely be left unsampled. In this study, we developed an algorithm to predict whether a given biopsy would find clinically significant prostate cancer using MRI data alone. Using a dataset of 11,095 biopsies collected from 711 patients, we developed a support vector machine for predicting the presence of clinically significant prostate cancer with a test set AUC of 0.72, precision of 0.877, and recall of 0.74.

1 Introduction

Prostate cancer is the most common newly diagnosed cancer and second most deadly cancer of American men (2). Transrectal ultrasound-guided (TRUS) MR fusion biopsy is a diagnostic procedure for prostate cancer in which potential targets for sampling are identified by radiologists on multiparametric MRI (mpMRI) of the prostate, and then ultrasound guidance is used to collect biopsies from those targets (6). This methodology has been demonstrated to be more sensitive than unguided biopsy. (3; 1). However, interpretation of prostate mp-MRI is challenging and has substantial inter-reader variability, suggesting a need for computer-based tools (7). In this work, we aim to develop a model for predicting whether or not clinically significant prostate cancer is likely to be found in a given biopsy location based on mpMRI.

[*]Department of Biomedical Engineering, Xi'an Jiaotong University
[†]Computational Integrated Diagnostics, Department of Radiological Sciences, University of California Los Angeles
[‡]Department of Bioengineering, University of California Los Angeles
[§]Department of Urology, University of California Los Angeles
[¶]Corresponding Author

32nd Conference on Neural Information Processing Systems (NeurIPS 2018), Montréal, Canada.

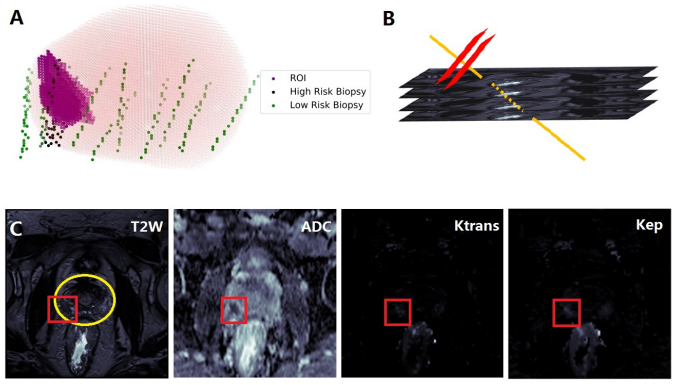

Figure 1: Our dataset consists of biopsy locations with associated Gleason scores and mpMRI studies with prostate and region of interest contours. A) Example prostate with illustrated biopsy locations. Biopsies were separated into two groups by Gleason score (GS > 3+3 and GS $\leq$ 3+3). mpMRI region of interest is also illustrated for comparison. B) Interpolation was used to create simulated MR planes perpendicular to the biopsy. C) The four MR data types from an example patient. The ROI referred to in A is highlighted in a red square; the yellow oval represents the prostate boundary.

2 Methods

2.1 Data acquisition

Data for a total of 759 patients was retrieved from clinical records retrospectively. All 759 patients underwent TRUS MR fusion biopsy using the Artemis guided biopsy system between 2010 and 2016. Before the biopsy procedure, each patient underwent multiparametric MR imaging, and a clinical radiologist identified regions of interest in the image to target for biopsy (ROIs). The patients then underwent TRUS biopsy, and 8-16 biopsy cores were retrieved from each patient's prostate using the sampling device. During sampling, the spatial coordinates of each retrieved core were recorded. Each core was then evaluated by a pathologist and assigned a primary and secondary Gleason score. For this study, we considered a biopsy core to contain clinically significant prostate cancer the Gleason score was greater than 3+3. Four types of imaging studies were retrieved from our Picture Archive and Communication System (PACS): T2-weighted images, apparent diffusion coefficient (ADC) maps, Kep maps, and Ktrans maps.

2.2 Preprocessing and Biopsy Modeling

Cores were included in our analysis unless they met at least one of three exclusion criteria: 1) MRI study was missing or invalid, 2) assigned Gleason grades were missing or invalid, or 3) the biopsy core was entirely outside of the prostate contour. After exclusion, 675 patients with a total of 9,384 biopsy cores remained. Of these retained cores, 981 (10.5%) were labeled as clinically significant.

Biopsy locations are represented by the Artemis system as a series of 20 points. For each point, we extracted a square region of MR data perpendicular to the biopsy at that point using 8-way linear interpolation between MR voxels. For any portions of the biopsy not contained within the prostate, mean padding was used to replace the excluded portion.

2.3 Feature Extraction and Selection

In order to represent heterogeneity along the length of a core, we initially split each core into two halves and computed features on each half; these features were then averaged together. We extracted a variety of features, including Haralick and wavelet textures (9; 8), statistical features (such as mean, variance, and percentile values) (4), and the histogram of oriented gradients (HOG) (5).

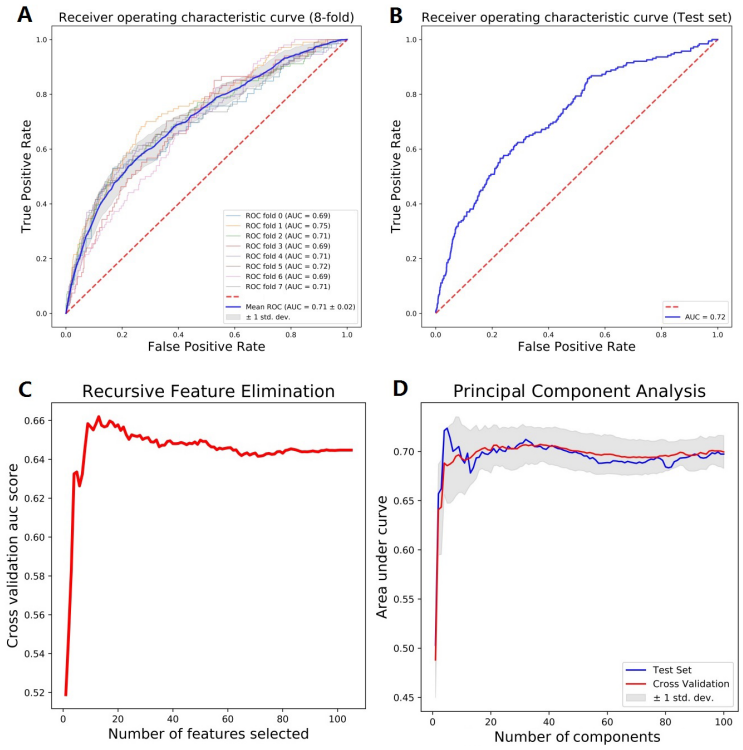

Figure 2: A) ROC curves plotted for the final eight-fold cross-validation with optimized parameters (537 patients) B) ROC curve for the test set (138 patients) C) Cross-validation AUC vs the number of features selected by RFE D) Cross-validation AUC vs the number of principle components selected using PCA

2.4 Dimension Reduction and Learning

Recursive feature elimination (RFE) and principle component analysis (PCA) were applied to reduce the dimensionality of the feature space. All features were normalized to zero mean and a unit variance. A bagging and balanced-weight support vector machine (SVM) with a radial basis function kernel was trained to classify clinically significant biopsy. A total of 539 patients (79.9%) were randomly selected to use as the training set while the remaining patients were used as a held-out test set. All parameters were optimized under eight-fold cross-validation on the training set. ROC curves were obtained and the area under the ROC curve (AUC) was used as the evaluation metric.

3 Results

As shown in Fig. 2, the mean AUC of the eight-fold cross validation was approximately 0.71 ± 0.02 with precision of 0.86 ± 0.02 and sensitivity of 0.72 ± 0.01, respectively, showing acceptable performance with small variance. The AUC of the test set is 0.72 with a precision of 0.87 and sensitivity of 0.74, and the f1-score of testing set is 0.80.

4 Conclusion

In this study, we built a classifier that predicts the existence of clinically significant prostate cancer at proposed biopsy locations using MR imaging data alone with acceptable performance. Our results demonstrate the potential for use of MR-based decision support tools in optimizing biopsy targeting for prostate cancer diagnosis. Substantial opportunities for further improvements exist that we continue to pursue. This includes the use of additional types of MR data (such as a calculated high b-value map and raw perfusion data) and the use of other types of models (such a deep learning models) for both feature extraction and prediction.

Acknowledgments

Wen Shi acknowledges support from the UCLA Cross-disciplinary Scholars in Science and Technology program. Karthik Sarma acknowledges support from NIH NCI F30CA210329 and the UCLA-Caltech Medical Scientist Training Program. This work was performed on hardware provided in part by an nVIDIA Academic Hardware Grant. This work was supported in part by grants from the National Cancer Institute: R21CA220352, R01CA218547, R01CA195505, and R01CA158627. The content is solely the responsibility of the authors and does not necessarily represent the official views of the National Cancer Institute or the National Institutes of Health.

References

[1] H. U. Ahmed, A. El-Shater Bosaily, L. C. Brown, R. Gabe, R. Kaplan, M. K. Parmar, Y. Collaco-Moraes, K. Ward, R. G. Hindley, A. Freeman, A. P. Kirkham, R. Oldroyd, C. Parker, and M. Emberton. Diagnostic accuracy of multi-parametric MRI and TRUS biopsy in prostate cancer (PROMIS): a paired validating confirmatory study. *The Lancet*, Jan 2017. ISSN 01406736. doi: 10.1016/S0140-6736(16)32401-1.

[2] K. J. L. Bell, C. Del Mar, G. Wright, J. Dickinson, and P. Glasziou. Prevalence of incidental prostate cancer: A systematic review of autopsy studies. *International journal of cancer. Journal international du cancer*, 137(7):1749–57, Oct 2015. ISSN 1097-0215. doi: 10.1002/ijc.29538.

[3] T. Golabek, W. Lipczynski, A. Czech, J. Kusionowicz, M. Zembrzuski, P. Dudek, T. Szopinski, and P. Chlosta. C89 Value of MRI-ultrasound fusion for guidance of targeted prostate biopsy. *European Urology Supplements*, 12(4):e1197, C89, Oct 2013. ISSN 15699056. doi: 10.1016/S1569-9056(13)61937-5.

[4] G. Litjens, O. Debats, J. Barentsz, N. Karssemeijer, and H. Huisman. Computer-Aided Detection of Prostate Cancer in MRI. *IEEE Transactions on Medical Imaging*, 33(5):1083–1092, May 2014. ISSN 0278-0062. doi: 10.1109/TMI.2014.2303821.

[5] P. Liu, S. Wang, B. Turkbey, K. Grant, P. Pinto, P. Choyke, B. J. Wood, and R. M. Summers. A prostate cancer computer-aided diagnosis system using multimodal magnetic resonance imaging and targeted biopsy labels. In C. L. Novak and S. Aylward, editors, *Medical Imaging 2013: Computer-Aided Diagnosis*, volume 8670, page 86701G. International Society for Optics and Photonics, Feb 2013. doi: 10.1117/12.2007927.

[6] S. Loeb, A. Vellekoop, H. U. Ahmed, J. Catto, M. Emberton, R. Nam, D. J. Rosario, V. Scattoni, and Y. Lotan. Systematic Review of Complications of Prostate Biopsy. *European Urology*, 64(6):876–892, Dec 2013. ISSN 0302-2838. doi: 10.1016/J.EURURO.2013.05.049.

[7] A. B. Rosenkrantz, L. A. Ginocchio, D. Cornfeld, A. T. Froemming, R. T. Gupta, B. Turkbey, A. C. Westphalen, J. S. Babb, and D. J. Margolis. Interobserver Reproducibility of the PI-RADS Version 2 Lexicon: A Multicenter Study of Six Experienced Prostate Radiologists. *Radiology*, page 152542, Apr 2016. ISSN 1527-1315. doi: 10.1148/radiol.2016152542.

[8] S. E. Viswanath, N. B. Bloch, J. C. Chappelow, R. Toth, N. M. Rofsky, E. M. Genega, R. E. Lenkinski, and A. Madabhushi. Central Gland and Peripheral Zone Prostate Tumors have Significantly Different Quantitative Imaging Signatures on 3 Tesla Endorectal, In Vivo T2-Weighted Magnetic Resonance Imagery. *Journal of Magnetic Resonance Imaging*, 36(1):213, 2012. doi: 10.1002/JMRI.23618.

[9] A. Wibmer, H. Hricak, T. Gondo, K. Matsumoto, H. Veeraraghavan, D. Fehr, J. Zheng, D. Goldman, C. Moskowitz, S. Fine, V. E. Reuter, J. Eastham, E. Sala, and H. A. Vargas. Haralick Texture Analysis of prostate MRI: Utility for differentiating non-cancerous prostate from prostate cancer and differentiating prostate cancers with different Gleason Scores. *European Radiology*, 25(10):2840, 2015. doi: 10.1007/S00330-015-3701-8.